

Evidence for polarons in iron pnictides of the $Ln-1111$ and $\mathcal{AE}-122$ families

Manuel Núñez-Regueiro

**Institut Néel, Centre National de Recherches Scientifiques & Université Joseph Fourier, BP166 cedex 9,
38042 Grenoble, France**

Examination of the electrical resistivities of iron pnictides shows that they can be accounted by conduction by polarons. Their activation energies show a linear behaviour with the critical temperatures of the spin density waves (SDW), T^* , as both vary with pressure. The slope matches the ratio SDW gap to T^* , while the intercept can be related to the transition temperature of the lattice distortion, T_θ . An adapted Landau free energy predicts the observed order of the transitions, according to which is higher, T^* or T_θ . Simple arguments favour combined Jahn-Teller antiferromagnetic bipolarons.

email: nunez@grenoble.cnrs.fr

71.38.-k ; 72.15.-v ; 74.90.+n ;

One of the main issues in superconductivity is the origin of the force binding electrons in pairs that condense into the quantum macroscopic state. High temperature superconductors were discovered following the belief that Jahn-Teller polarons¹ could render strong binding forces, though the precise origin of the pairing interaction in cuprates still remains controversial. A new opportunity has now appeared with the report of superconducting transition temperatures up to ~56K in compounds with iron in tetrahedral coordination^{2, 3, 4, 5}. As in cuprates, the ground state of the mother compounds exhibits antiferromagnetic order⁶, whose residual interactions on doping are presently held responsible for the pairing. However, in contrast with cuprates it is an itinerant antiferromagnetic state of the spin density wave type (SDW)⁷. However, the lattice distortion⁸ that is also always present in the ground state nor its relation to the SDW are presently understood. Besides, the reason why the phase transition towards the antiferromagnetic state is always second order, while the lattice distortion can be second order for *LnFeAsO* (*Ln-1111*), where *Ln* is a lanthanide, or first order for *ÆFe₂As₂* (*Æ-122*), where *Æ* is an alkaline-earth, remains also a puzzle. More basically, the "bad metal" electrical resistance of these materials at high temperatures, lacks a coherent and straightforward interpretation.

Here it is shown that the electronic transport properties of the mother compounds can be naturally explained assuming the existence of polarons at high temperatures, whose cooperative ordering can bring about the lattice distortion. The analysis of the correlation obtained between the activation energy of the polarons and the transition temperature towards the SDW, T^* , leads to the existence of antiferromagnetic bipolarons. The strong coupling between the lattice and antiferromagnetic transitions is analyzed and the order of the phase transitions deduced, in agreement with experiment.

Band structure calculations for the undoped *LnFeAsO* (*Ln-1111*) oxypnictides yield⁹ two dimensional cylindrical hole and electron Fermi surfaces that are prone to nesting,

rendering an itinerant antiferromagnetic ground state in the form of a SDW⁷, as is found experimentally⁶ at T^* . The archetype for this type of phase transition is chromium metal¹⁰, which develops a SDW at $T^*=312\text{K}$. However, the dependence of the electrical resistance of chromium, metallic above and below T^* , though common to most of SDW compounds (e.g. Cobaltites¹¹), is strikingly different to the dependence observed in pnictides. As a tetragonal to orthorhombic lattice distortion (TOLD) is also observed⁸ at a transition temperature $T_0 > T^*$, it is basic to take into account possible electron-lattice coupling effects. As the crystal field effect of the arsenic tetrahedron on the five degenerate $3d Fe$ levels can explain several of the $Ln-1111$ properties¹², it is natural to refer to materials with similar configurations, such as manganites¹³. In fact, the resistivity curve on Fig 1(a) bears many resemblances with the behaviour observed in those materials¹³, where the transport at high temperatures is attributed to small Jahn-Teller polarons with a $\rho \sim T \exp(E_a/k_B T)$ temperature dependence, ρ being the resistivity, E_a an activation energy, and k_B the Boltzmann constant. Applying the assumption of polaronic transport on pnictides, the subsequent Arrhenius plot of Fig 1(b) allows determining E_a for the $Sm-1111$ oxypnictide. Although this sample is polycrystalline an identical behaviour is observed for the monocrystalline $Sr-122$ pnictide, Fig. 1(c) and Fig 1(d), thus confirming that it is an intrinsic feature. E_a can thus be obtained from the Arrhenius of the published data on $Ln-1111$ and $\mathcal{A}E-122$ pnictides electrical resistivity data, while T^* can be determined from the peak of the derivative of the resistivity with respect to temperature, $d\rho/dT$. Both parameters are plotted on Fig 2 a and Fig 2 b as a function of the basal lattice parameter resulting in a linear correlation for all the rare earths (with the exception of La , whose doped samples also have an anomalously low superconducting transition temperature) on the $Ln-1111$ plot and for Ca and Sr on the $\mathcal{A}E-122$ plot. Remarkably, the E_a has a magnitude comparable to the Fe $3d$ level separation in the distorted tetrahedral field¹². It is tempting to associate these polarons to a Jahn-Teller (JT) effect, since, as shown on Fig 3d, there is

splitting of a doublet when the TOLD takes place. JT polarons may exist above T_0 , when they would condensate into a permanent TOLD, through, presumably, a cooperative JT transition¹⁴. Alternatively, polarons have been recently¹⁵ predicted in pnictides, although based on the highly polarizable As $4p$ states, and not on crystal field JT effects.

The optimal way to determine the relationship between E_a and T^* is from pressure measurements on the same sample¹⁶, as in such a way the differences between different samples (defects, impurities, etc.) are avoided. Up to date reported pressure measurements are found on Sm and La -1111 and Ca , Sr and Ba -122. The activation energy and the transition temperature for each pressure are now extracted from the published data, and plotted one against the other on Fig 2c and Fig 2d, each point being one different pressure. The dependences are extremely linear, i.e. $E_a = \varepsilon + \alpha T^*$, with the same slope α for each family materials but different intercept energy ε for each compound. Referring once more to manganites, it is useful to propose a band picture for the strongly coupled electron-phonon system (similar to the one on Fig. 1 of Ref. 17) including narrow polaronic bands (Fig 3 c). The point here is that, contrary to manganites, there is no real gap in pnictides. However, precursor fluctuations of the SDW, rendering a pseudogap above T^* , are currently expected (due to a nematic phase¹⁸ or dimensionality fluctuations¹⁹). Also, a pseudogap has been used to explain the anomalous magnetic susceptibility²⁰ of undoped pnictides at $T > T^*$. Thus, here a pseudogap Δ^* replaces the band gap of manganites, with the smaller polaronic gap between electron and hole polaron bands. This latter gap ε_0 can be obtained through thermoelectric power measurements^{13,17}. The thermopower of small polaronic systems is similar to that of band semiconductors, governed by thermal activation of carriers across a small barrier and thus a function of the inverse temperature: $S = \frac{k_B}{e} \left(\frac{E_S}{k_B T} + b \right)$ where S is the thermopower, E_S is an activation energy ($=\varepsilon_0$), e the electronic charge and b other, negligible terms. The value

of the activation energy E_S for several *Ln-1111* samples is thus determined from the measured thermopowers through the plot on Fig 3 a. It can now be compared to the intercept ε (Fig 3 b). To a good approximation $\varepsilon \approx E_S = \varepsilon_0$, i.e. as a first estimate the intercept ε corresponds to the polaronic gap ε_0 .

Analyzing now the activation energy of the electrical resistivity, for small polarons it is, $E_a = \varepsilon_0 + W_H - J$, where W_H is one half^{13,21} of the polaron formation energy E_P , and J the transfer integral. As from the diagram on Fig 4c $\Delta^* = \varepsilon_0 + E_P$, then $E_a = \frac{\varepsilon_0 + \Delta^*}{2} - J$. The

relation between the gap and the transition temperature in a mean field approximation is

$$\Delta = 1.75k_B T^*, \text{ and more generally } \Delta^* = \delta k_B T^*. \text{ Thus, } E_a = \frac{\varepsilon_0 + \delta k_B T^*}{2} - J \text{ (1).}$$

In this way the linear dependence of E_a on T^* can be explained, with the slope α related to the ratio gap to critical temperature, δ . However, from this expression the intercept ε should be $\sim E_S/2 = \varepsilon_0/2$, when it is clear from Fig 4b, that $\varepsilon \approx E_S = \varepsilon_0$. Although ε_0 can be expected to change with pressure, this variation may be included into the actual error of determination, i.e. 20%. The ratio δ of the gap to the critical temperature is obtained from the reported optical absorption gap measurements for *Ln-1111*²² and *Æ-122*²³ materials, yielding $\delta_{1111} \approx 1.04 \pm 0.4$ and $\delta_{122} \approx 1.75 \pm 0.05$. These values are almost identical to the slopes $\alpha_{1111} = 1.16 \pm 0.1$ and $\alpha_{122} = 1.60 \pm 0.06$, while according to formula (1) they should be twice their value. Thus, the precedent analysis agrees qualitatively and quantitatively with experiments if the factor $\frac{1}{2}$ is eliminated, i.e. if electronic transport is performed by two polarons simultaneously, in a first approximation bipolarons. This $\frac{1}{2}$ factor that points towards bipolarons appears in the formulas through the relation that states that the hopping of polarons costs half their energy of formation, relation that has been recurrently time-tested^{13,21}.

It is interesting to note that while the intercept ε for the *Ln-1111* compounds is positive, that for *Ba-122* is also positive but very small, and is negative for *Sr* and *Ca*,

meaning that polarons are deep inside the Fermi sea for the later two. It is reasonable to assume that, while long lifetime polarons (*Ln-1111* and eventually *Ba-122*) can trigger a TOLD before the appearance of the SDW, i.e. $T_0 \geq T^*$, those with a very short lifetime through strong hybridization (*Sr*, *Ca*) will have very low or nil condensation temperatures and in this case $T^* \gg T_0$. In other words, the intercept ε should be related to the part of the activation energy that is due to the JT deformation, positive for the *Ln-1111* compounds and thus increasing their stability, while for the *Æ-122* it is almost zero or negative and decreasing their stability.

A Landau free energy analysis is useful here to study the scenario of the interrelation between the transitions, in particular the order of the phase transformations. According to specific heat measurements, the phase transitions are of second order for the *Ln-1111* ($\varepsilon > 0$) and *Ba-122* ($\varepsilon \sim 0$)²⁴ (although for this last compound this seems to be sample dependent²⁵, as would be expected due to its very small ε), and of first order for *Sr-122*²⁶ and *Ca-122*²⁷. The Landau free energy for the system reads

$$F = a(T - T^*)\eta_{SDW}^2 + a'(T - T_0)\eta_{LD}^2 + b\eta_{LD}\eta_{SDW}^2 - c\eta_{LD}^2\eta_{SDW}^2 + d\eta_{SDW}^4 + d'\eta_{LD}^4 \quad (2)$$

where a, a', b, c, d, d' are parameters, T^* and T_0 the uncoupled transition temperatures and η_{LD} and η_{SDW} are the order parameters for the TOLD and the SDW, respectively. The first, second, fifth and sixth terms are standard. The third linear-quadratic one is a particular coupling allowed by symmetry, as the wavevector for the TOLD is twice the one of the SDW (this term is common in spin-Peierls systems) and the fourth one explicits a strong favorable coupling that is assumed between the two transitions based on the same bands. The coupling translates the fact that due to the SDW transition, the bands degenerate at M and Γ split⁹, as in a band JT transition²⁸. Solving first for $T_0 \geq T^*$, putting as for the *Ln-1111* case $T_0 = 155K$ and $T^* = 90K$ (the expected transition temperature from the ratio $\delta_{1111}/1.75$ if mean field holds), both transitions are second order and the actual transitions temperatures $T_0 = 155K$

and $T^* = 145K$, in agreement with measurements (Fig 4 a), i.e. due to the coupling with the TOLD the SDW transition increases in temperature. While if the SDW appears before the TOLD, i.e. $T^* > T_0$, putting tentatively " $T_0 \sim 0K$ and " $T^* = 200K$, as expected for *Sr-122*, the SDW transition is second order but the TOLD transition is now first order, as is precisely found experimentally²⁹, with $T^* = 200K$ and (Fig. 4 b) $T_0 = 185K$, very near to the observed values (the same a, a', b, c, d, d' have been used for both calculations). The order of the phase transitions is thus the immediate consequence of the expected by symmetry linear-quadratic coupling of the SDW-TOLD states.

A structure for the bipolaron would be nearest neighbours polarons coupled antiferromagnetically (Fig 4c), in a minimalist version of the TOLD-SDW. For *Sr-122* and *Ca-122* compounds, the energy gain from the antiferromagnetic coupling will stabilize the otherwise unstable polarons, while the distortion is the only way to create a magnetic moment ($\sim 0.35\mu_B$, Ref.12) on the Fe atom. The supposition of antiferromagnetic bipolarons would also justify the existence of a pseudogap at $T > T^*$. It must be noted here that these are not standard bipolarons, as the latter are singlet coupling of two polarons that have no localized spin. Transport at $T > T^*$ would be performed through antiferromagnetic bipolarons (BP) and free carriers (FC). FC would have a short constant mean free path due to scattering against the disordered BP and a comparatively small T dependence, while the certainly pinned BP can be excited through E_a to FC and re-pinned elsewhere, i.e. $\rho_{BP} \sim T \exp(E_a/k_B T)$. Below T^* , BP order into the coupled TOLD-SDW, while the ungapped FC would have a mean free path increasing with the TOLD-SDW gap temperature dependence.

In conclusion, it is shown that polaronic formation can explain the "bad metal" electrical resistivity of the mother compounds of the superconducting iron pnictides. From the analysis of the variation with pressure of the activation energy of the polarons and the SDW transition temperature, it is concluded that they are coupled in pairs of antiferromagnetically

coupled Jahn-Teller bipolarons. Bipolarons in the mother compounds can be crucial in the understanding of the pairing mechanism of pnictides^{30,15}, if their existence were attested also in the doped materials. Besides, the fact that both imbricated transitions yield bipolarons strongly suggests that pairing should contain elements of both interactions. Finally, it is also demonstrated that the order of the SDW and TOLD transitions is the consequence of their particular linear-quadratic coupling within a Landau free energy analysis.

The author acknowledges Gastón Garbarino, Marie-Bernardette Lepetit, José Emilio Lorenzo, Pascal Quemerais and Rubén Weht for help during analysis, and Blas Alascio, Michel Avignon, Claudine Lacroix, Pierre Monceau and Julius Ranninger for fruitful discussions.

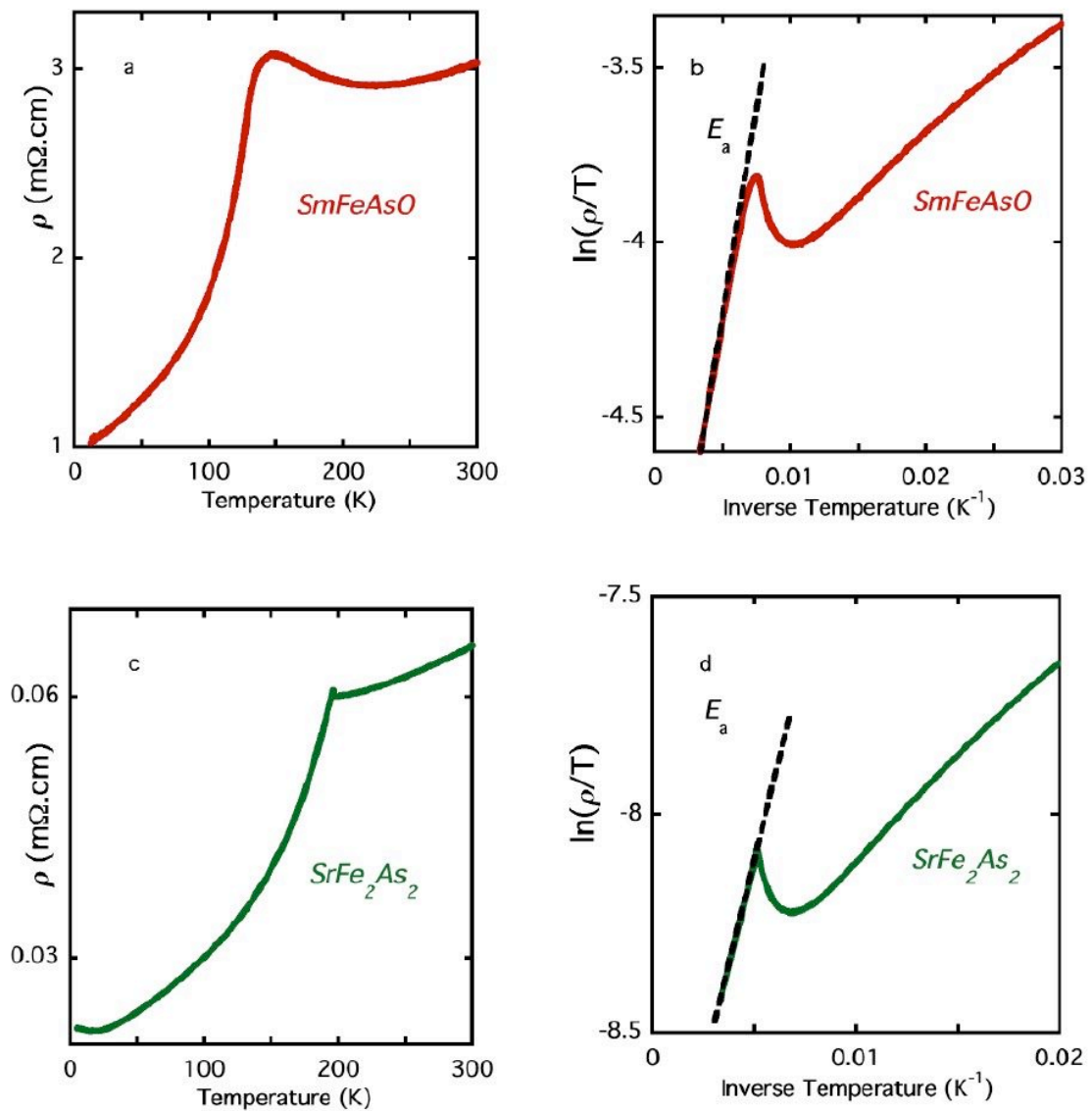


Figure 1. (a) Electrical resistance of a $SmFeAsO$ sample³⁸. (b) Data of (a) plotted in an Arrhenius plot (logarithm of resistivity/temperature versus inverse temperature) in order to determine the activation energy E_a due to small polaron transport (c) Electrical resistivity of a $SrFe_2As_2$ sample³¹ (d) Same as (c) for the $SrFe_2As_2$ sample.

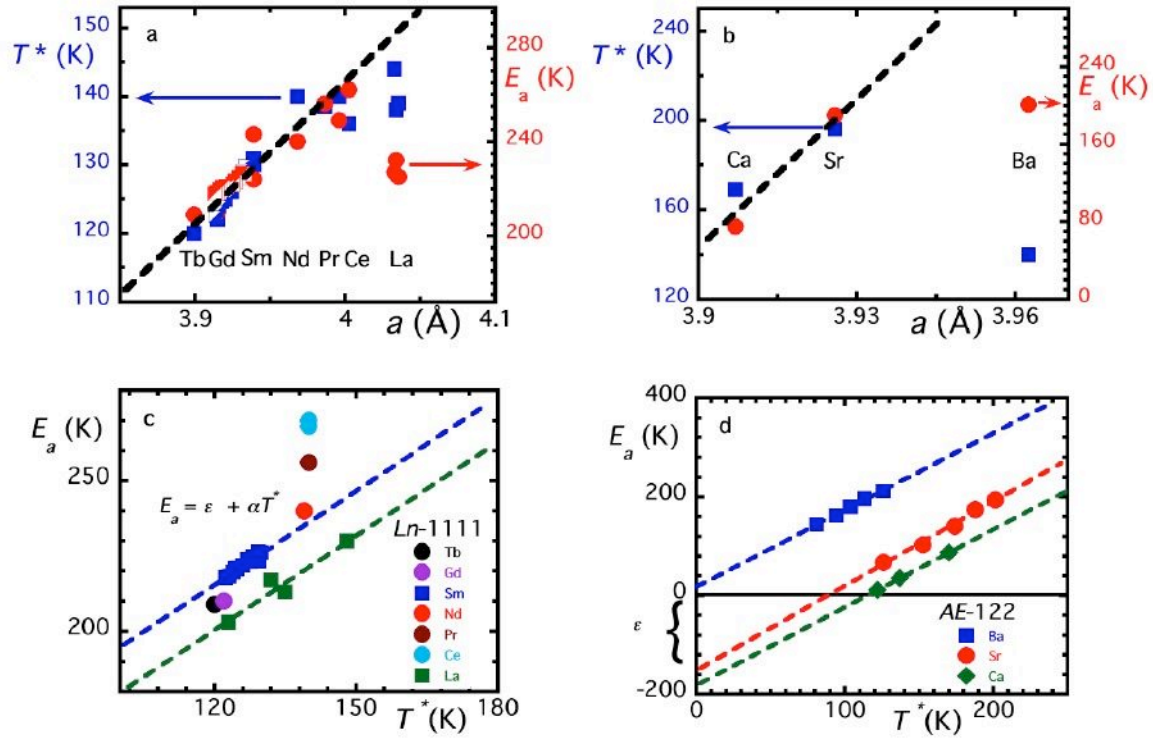


Figure 2 (a) Transition temperature T^* to the SDW state, as determined by the peak of the derivative of the electrical resistance, together to the activation energy E_a , determined as in Fig 1 b, for different published $Ln-1111$ compounds as a function of the basal lattice parameter, La^2 , 3^{3233} , Gd^34 , Ce^{3536} , Tb^{37} , Nd^{36} , Gd^{36} , Pr^{36} and $Sm^{38,39}$. The data shown with half-squares corresponds to structural and electrical resistance measurements on $Sm-1111$ under pressure⁴⁰. (b) Same as (a) for the $AE-122$ family, Ba^5 , Sr^{31} , Ca^{41} . (c) Plot of the activation energy as a function of the SDW transition temperature. Only $Sm-1111$ ⁴⁰ and $La-1111$ ⁴² have been measured under pressure where each point corresponds to one pressure. (d) Same as (c) for the $AE-122$ compounds, Ba^{43} , Sr^{44} , Ca^{41} . The dependences are surprisingly linear and parallel within each family of compounds.

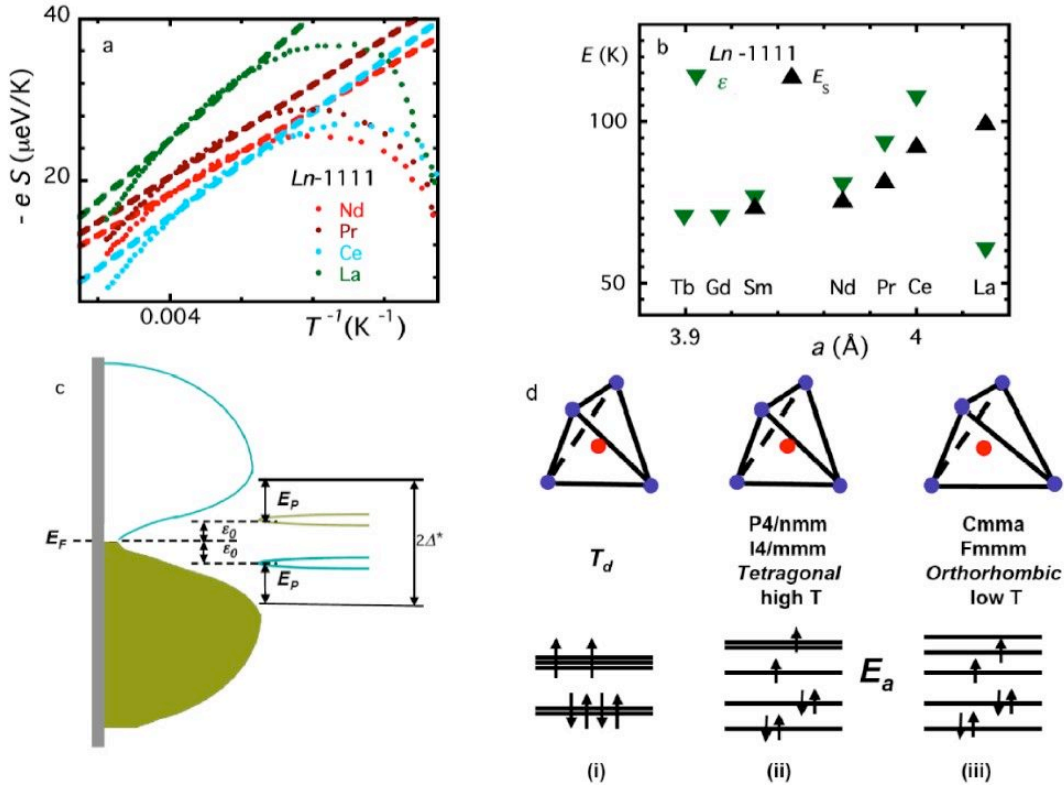


Figure 3 (a) Thermopower of *Ln-1111* compounds to determine the activation energy E_S . (b) Comparison of the intercept ε from Fig. 2 c (the value for compounds where there are no pressure measurements, were obtained using the same slope as for *Sm-1111* and *La-1111*) to E_S as a function of the basal lattice parameter. For the Sm^{38} , Nd^{32} , Pr^{32} and Ce^{32} compounds the agreement is better than 20%. (c) Schematic band diagram for pnictides. The density of states derived from the conduction bands has a dip corresponding to the pseudogap $2\Delta^*$ that exists above T^* . Two narrow polaronic bands are shown, separated by an energy $2\varepsilon_0=2E_S$, corresponding to hole or electron polarons. E_P is the formation energy of a polaron. (d) Levels at the *Fe* site for (i) a tetrahedral environment, (ii) the tetragonal high temperature structure and (iii) the low temperature orthorhombic structure⁴⁵. The filling explains the JT effect, as the splitting of the degenerate level induced by the orthorhombic distortion causes an energy gain ($\varepsilon>0$), in the case of the *Ln-1111* and *Ba-122* compounds (for the other 122 materials the doublet and the singlet are probably inverted).

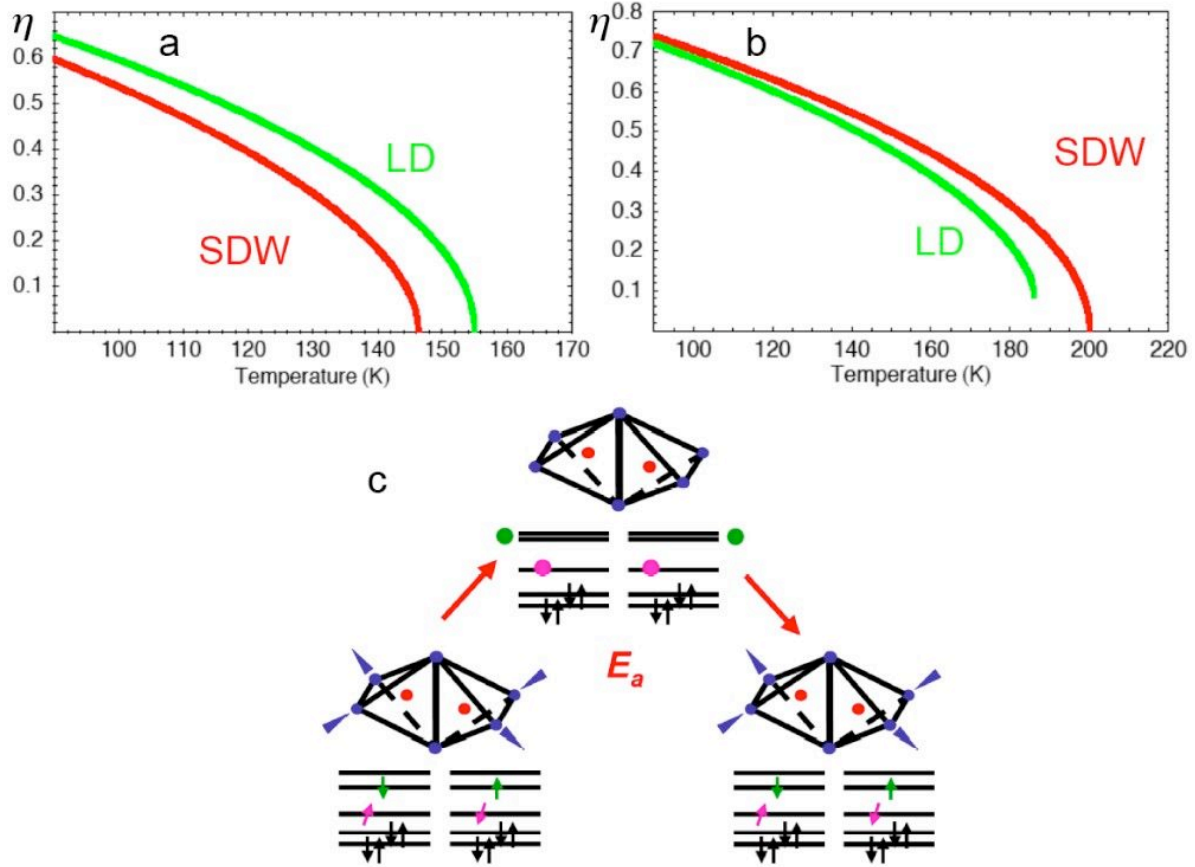


Figure 4 (a) Temperature dependence of the order parameter of the SDW (red) and the TOLD (green) according to the Landau free energy (1) for uncoupled transition temperatures $T_0(=155\text{K}) > T_L^*(=90\text{K})$, both transitions are of second order and $T_0=155\text{K}$ and $T_L^*=145\text{K}$. (b) Same as (a) but for the case $T_L^*(=200\text{K}) > T_0(=0\text{K})$. This is the strictest case, higher T_0 will give almost identical final transition temperatures, but for all $T^* > T_0$ cases the TOLD transition will be of first order. (c) Possible structure of the antiferromagnetic bipolaron and its conducting mechanism. The energy levels and spin disposition have been taken from Ref. 12. The bipolarons are in the deformed state and can be excited to the undeformed state through the excitation energy E_a , that frees the uppermost electrons (green circles) for a FC conduction though they are later pinned down to a new bipolaron state.

References

- 1 J.G. Bednorz, and K.A. Müller, *Zeit. Phys. B* 64, 189 (1986)
- 2 Y. Kamihara, T. Watanabe, M. Hirano and H. Hosono, *Journal of the American Chemical Society* **130**, 3296 (2008).
- 3 H. Takahashi, K. Igawa, K. Arii, Y. Kamihara, M. Hirano and H. Hosono *Nature (London)* **453**, 376 (2008).
- 4 X.H. Chen, T. Wu, G. Wu, R.H. Liu, H. Chen and D.F. Fang, *Nature (London)* **453**, 761 (2008).
- 5 M. Rotter, M. Tagel, D. Johrendt, *Phys. Rev. Lett.*, 101, 107006 (2008).
- 6 C. De la Cruz et al., *Nature* 453, 899-901 (2008)
- 7 A.W. Overhauser, *Phys. Rev.* 128, 1432 (1962)
- 8 T. Nomura et al., *Superconductor-Science-and-Technology*, 21, 125028 (2008)
- 9 F. Ma and Z-Y.Lu, *Phys. Rev. B* 78, 033111 (2008)
- 10 E. Fawcett et al., *Rev. Mod. Phys.* 66, 25 (1994)
- 11 G. Garbarino, M. Núñez-Regueiro, M. Armand and P. Lejay, *Europhys. Lett.* 81, 47005- (2008)
- 12 J. Wu, P. Phillips and A.H. Castro Neto, *Phys. Rev. Lett.* 101 126401 (2008)
- 13 M.B. Salamon and M. Jaime, *Rev. Mod. Phys.* 73, 583 (2001)
- 14 G.A. Gehring and K.A. Gehring, *Rep. Prog. Phys.* 38, 1 (1975)
- 15 M. Berciu, I. Efimov and G.A. Sawatzky, *ArXiv* 0811.0214v1
- 16 B. Lorenz et al., *Phys. Rev. B* 63, 1444405 (2001).
- 17 M. Jaime, M.B. Salamon, M. Rubinstein, R.E. Treece, J.S. Horwitz and D.B. Chrisey, *Phys. Rev. B* 57, 11914 (1996)
- 18 C. Fang, H. Yao, W.F. Tsai, J.P. Hu and S.A. Kivelson, *Phys. Rev. B* 77 224509 (2008)
- 19 D.C. Johnston, K. Maki and G. Grüner, *Sol. State Comm.* 53, 5-8 (1985)
- 20 G.M. Zhang, Y.H. Su, Z.Y. Lu, Z.Y. Weng, D.H. Lee and T. Xiang, , *ArXiv* 0809.3874 (2008)
- 21 I.G. Austin, and N.F. Mott, *Adv. Phys.* 18, 41 (1969)
- 22 C. Wang, et al., *Europhys. Lett.* 83, 67006 (2008)
- 23 W. Hu et al., *Phys. Rev. Lett.*, 101, 257005(2008)
- 24 M. Rotter et al., *Phys. Rev. B* 78, 020503 (2008)
- 25 Q. Huang et al., *Phys. Rev. Lett.* 101, 257003(2008)
- 26 G.F. Chen et al., *Phys. Rev. B* 78, 224512(2008)
- 27 N. Ni et al, *Phys. Rev. B* 78, 014523 (2008)
- 28 J. Labbe and J. Friedel, *J. de Phys.* 27, 153 (1965)
- 29 Y. Zhao, et al., *Phys. Rev. B* 78, 140504 (R) (2008)
- 30 R. Micnas, J. Ranninger and S. Robaszkiewicz, *Rev. Mod. Phys.*, 62, 113 (1990)
- 31 G.F.Chen. et al., *ArXiv* 0806.2648(2008)
- 32 M.A. McGuire et. al., *Phys. Rev. B* 78, 094517 (2008)
- 33 A.S. Sefat, A. S., *Phys. Rev. B* 78, 104505 (2008)
- 34 C. Wang et al., *Europhys. Lett.* 83, 67006 (2008)
- 35 G.F. Chen et al., *Phys. Rev. Lett.* 100, 247002 (2008)
- 36 M. A. McGuire et al., *New J. Phys.* 11, 025011(2009)
- 37 L.J. Li et al., *Phys. Rev. B* 78, 132506 (2008)
- 38 M. Tropeano et al., *ArXiv:0809.3500*.
- 39 Y.K. Li et al., *Phys. Rev. B* 79, 054521 (2009)
- 40 G. Garbarino et al., to be published

-
- 41 M.S. Torikachvili, S.L. Bud'ko, N. Ni and P.C. Canfield, Phys. Rev. Lett., 101, 057006 (2008)
- 42 H. Okada. et al., to be published J. Phys. Soc. Jpn.77 (2009)
- 43 H. Fukuzawa- et al., J. Phys. Soc. Jpn. Vol.77 105004, (2008).
- 44 H. Kotegawa H. Sugawara and H. Tou, J. Phys. Soc. Jpn. 78 (2009) 013709
- 45 From the Bilbao Crystallographic Server, <http://www.cryst.ehu.es/>